# Tunable Integrated Electro-Optic Wavelength Filter With Programmable Spectral Response

Harald Herrmann,  Kai-Daniel Büchter,  Raimund Ricken, and  Wolfgang Sohler

*Abstract*—**In this paper, we report on an integrated optical wavelength filter device in LiNbO$_3$. A sequence of individually addressable polarization converters enables programmable spectral response and continuous wavelength tunability. Wavelength-selective polarization conversion is obtained using in-phase and quadrature-driven electro-optic converters. A model based on coupled-mode analysis is presented that allows to determine the filter performance. Examples of tailoring the spectral response to obtain strong sidelobe suppression and flat-top responses are discussed. Predicted theoretical results are confirmed by experiments. A 2.3 nm wide bandpass filter with more than 20 dB sidelobe suppression and a tuning range of about 20 nm are demonstrated. Moreover, even a flat-top characteristics with 4.9 nm bandwidth and about 15 dB sidelobe suppression could be demonstrated with the same device.**

*Index Terms*—**Butterworth filters, electro-optic filters, integrated optics, lithium niobate, optical waveguide filters, programmable filters.**

## I. INTRODUCTION

WAVELENGTH filters are key components for applications involving optical systems, e.g., in optical communications or optical instrumentation. For each of these applications, special demands on filter characteristics have to be met. While bandpass characteristics with a strong rejection outside of the passband are sometimes required for certain purposes, wavelength tunability and/or an especially tailored spectral response are important for many other applications.

Among existing wavelength filters integrated optical versions play a key role in fiber-optic systems (see, e.g., [1]). In recent years, various types of integrated optic filters have been demonstrated, and some of these are now available as commercial components.

A class of integrated optical wavelength filters relies on a wavelength-selective polarization conversion in LiNbO$_3$. The conversion can either be induced by an acoustical wave, a static strain-induced grating, or via the electro-optic effect. For the latter, a periodic electric field is necessary to satisfy the phase-matching requirement, thus allowing efficient polarization conversion [2], [3].

When such electro-optic filters are operated with a constant voltage applied to all converter electrodes, a fixed sinc$^2$-like

spectral filter response is observed. We have demonstrated for the first time how to modify such filters to obtain a programmable spectral response [4]. In this case, the filter is composed of a series of integrated electro-optic polarization converters. A tailoring of the spectral response is enabled by individually addressing the different converters. More recently, Ping *et al.* have applied the same principle to demonstrate apodized spectral responses [5]. Moreover, they even incorporated this structure into an IC polarization-independent matched bandpass filter [6].

In this contribution, we will show that an advanced electrode design using in-phase and quadrature electrodes enables broad tunability and flexible passband tailoring. We emphasize that, besides sidelobe suppression already shown in [5], even more sophisticated spectral responses like flat-top characteristics can be realized. Moreover, tunability of such filters will be discussed.

In Section II, the principle of operation and the device structure is described. Modeling of spectral characteristics and tuning properties are discussed in Section III. In Section IV, details on the sample fabrication are given, followed by a discussion of the experimental results in Section V.

## II. DEVICE STRUCTURE AND PRINCIPLE OF OPERATION

In X-cut LiNbO$_3$, a polarization conversion of Y-propagating light can be induced by a periodic electric field parallel to the Y-axis. In a Ti-indiffused optical waveguide, this corresponds to a coupling of TE- and TM-polarized modes via the $r_{51}$ component of the electro-optic tensor [2]. Coupling along the $z$-direction of the coordinate system (which corresponds to the Y-crystalline axis) can be described using the coupled-mode theory with complex amplitudes $A_{TE}$ and $A_{TM}$ of the TE- and TM-polarized modes

$$\frac{dA_{TE}}{dz} = i\kappa A_{TM} \exp(-i\Delta\beta z)$$
$$\frac{dA_{TM}}{dz} = i\kappa A_{TE} \exp(+i\Delta\beta z) \qquad (1)$$

with the phase mismatch term $\Delta\beta = \beta_{TM} - \beta_{TE} - (2\pi)/\Lambda$. The variables $\beta_{TE}$ and $\beta_{TM}$ are the wavenumbers of the TE- and TM-polarized modes, respectively.

The coupling coefficient $\kappa$ is given by [2]

$$\kappa \approx \frac{4\pi}{\lambda}\sqrt{n_{TE}^3 n_{TM}^3}\, r_{51}\Gamma\frac{U}{\Lambda} \qquad (2)$$

with $n_{TE}$ and $n_{TM}$ being the effective indexes of the TE- and TM modes, respectively, $U$ is the applied voltage, and $\Lambda$ is the periodicity of the electrode pattern. $\Gamma$ is the normalized overlap of the electrical field with the two optical fields.
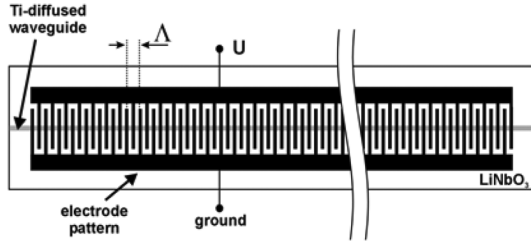
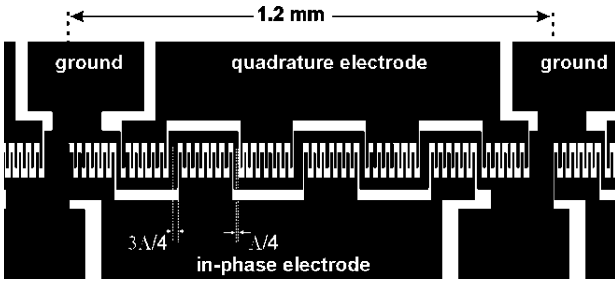Fig. 1.  Electro-optic polarization converter with homogeneous coupling.



Fig. 2.  Details of an electrode section with in-phase and quadrature electrodes.

For efficient conversion, phase matching is required, i.e., $\Delta\beta \approx 0$ must be fulfilled. In effect, the difference in wavenumbers of the TE- and TM polarized modes must be compensated by the periodicity of the electric field. As a direct consequence, the wavelength at which phase matching is obtained is determined by the period of the comb-like electrode pattern (see Fig. 1) on top of the waveguide.

In the special case where the coupling strength along the interaction length is constant (i.e., $\kappa(z) = \text{const.}$), (1) can be solved analytically [2]. The spectral response of a device with length $L$ is proportional to $\text{sinc}^2(\sqrt{\kappa^2 + (\Delta\beta/2)^2}L)$. For arbitrary functions of $\kappa(z)$, (1) has to be solved numerically to determine the spectral characteristics. However, for a first approximation, the spectral response can be estimated from the square of the Fourier transform of $\kappa(z)$ [7]. Therefore, it becomes evident that a tailoring of the spectral characteristics is possible via a proper design of the coupling strength $\kappa(z)$. Similar schemes for tailoring a spectral response have already been demonstrated for instance to design integrated acousto-optical filters [8], [9] or Bragg-type reflectors [10].

The idea of this study is to apply this principle to an electro-optic polarization converter to realize a programmable spectral filter by using a sequence of interdigital electrode sections, which can be individually addressed with different voltages. Moreover, even tuning of the filter is possible—as will be outlined in Section III—if each section is composed of two interleaved electrode structures that are shifted by a quarter of a period, called in-phase and quadrature electrodes. The device uses $N$ of such electrode sections. Details of an electrode section, which is about 1.2 mm long, are shown in Fig. 2. The electrodes form a sequence of finger pairs with a periodicity of $\Lambda$. In-phase and quadrature interdigital electrodes alternate after 6 or 7 finger pairs with a shift of $\Lambda/4$ in between. Devices with such electrode structures have already been successfully used as distributed polarization-mode dispersion compensators [11].

The structure is designed to provide full freedom in the design of $\kappa(z)$. The overall device is driven by $2N$ voltages $U_{i1}, \ldots, U_{iN}$ and $U_{q1}, \ldots, U_{qN}$ applied to the in-phase and quadrature electrodes, respectively.

## III. MODELING

To obtain a desired spectral response, the corresponding $2N$ drive voltages have to be determined. Starting from a given spectral response, this can be done by first determining the corresponding coupling strength function $\kappa(z)$ using an inverse scattering formalism [13], and subsequently discretizing the result into $N$ intervals according to the number of electrode sections. However, applying the inverse scattering method is relatively difficult and restricted to transmission characteristics which can be reasonably well approximated to rational function expressions [14]. Therefore, we have chosen another way to determine the voltage set. We start with trial functions and optimize them until we achieve the desired result. Such trial functions can be obtained either from an inverse Fourier transformation of the desired spectral response or by using well-known window functions that are frequently applied in apodization schemes [10].

The optimization process requires the calculation of the spectral response for a given $\kappa(z)$ discretized into $N$ sections. Each section of the filter can be treated as an electro-optic converter with homogeneous coupling. For a device with the interaction length $L$ and $N$ sections of equal length $l = L/N$, a formalism can be applied, which is analogous to the Jones matrix formalism in conventional optics. The amplitudes $A_{\text{TE}}$ and $A_{\text{TM}}$ at the output port of the device can then be calculated as

$$\begin{pmatrix} A_{\text{TE}} \\ A_{\text{TM}} \end{pmatrix} = \left\{ \prod_{n=1}^{N} \begin{bmatrix} P_n \exp(-i\beta_{\text{TM}}l) & -iQ_n \exp(-i\beta_{\text{TM}}l) \\ -i\bar{Q}_n \exp(-i\beta_{\text{TE}}l) & \bar{P}_n \exp(-i\beta_{\text{TE}}l) \end{bmatrix} \right\} \times \begin{pmatrix} A_{\text{TE},0} \\ A_{\text{TM},0} \end{pmatrix} \tag{3}$$

with $A_{\text{TE},0}$ and $A_{\text{TM},0}$ being the amplitudes of the TE and TM modes, respectively, at the input of the section. The overall Jones matrix is given by the product of the matrices of the individual sections. The elements of these matrices can simply be derived from the analytic solution of (1) with homogeneous coupling. One obtains

$$P_n = \exp\left(-i\frac{\Delta\beta}{2}\cdot l\right)\left[\cos\left(\frac{l}{2}\sqrt{4\kappa_n^2 + \Delta\beta^2}\right) \right.$$
$$\left. + \frac{i\Delta\beta}{\sqrt{4\kappa_n^2 + \Delta\beta^2}}\sin\left(\frac{l}{2}\sqrt{4\kappa_n^2 + \Delta\beta^2}\right)\right]$$
$$Q_n = \frac{2\kappa_n}{\sqrt{4\kappa_n^2 + \Delta\beta^2}}\sin\left(\frac{l}{2}\sqrt{4\kappa_n^2 + \Delta\beta^2}\right)$$
$$\times \exp\left(\frac{-i\Delta\beta}{2}\cdot l\right) \tag{4}$$

where $\bar{P}_n$ and $\bar{Q}_n$ are the complex conjugates of $P_n$ and $Q_n$, respectively, and $\kappa_n$ is the coupling strength within the $n$th section. The local coupling strength $\kappa_n$ is proportional to the local electric field strength, and thus to the drive voltages $U_{\text{in}}$ and
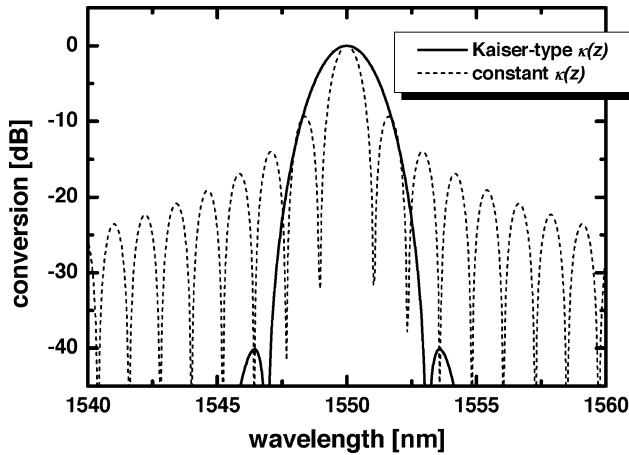
Fig. 3. Calculated spectral responses assuming a coupling strength function according to a Kaiser-type window function discretized into 20 sections. For comparison, the dashed line shows the response assuming a homogeneous coupling strength.

$U_{qn}$. The in-phase and quadrature parts are taken into account by assuming an effective drive voltage

$$U_{\text{eff},n} = \sqrt{U_{\text{in}}^2 + U_{\text{qn}}^2} \tag{5}$$

with an additional relative phase shift

$$\Delta\Phi_n = \arctan(U_{\text{qn}}/U_{\text{in}}). \tag{6}$$

As an example, the development of a filter with strong sidelobe suppression is presented. Starting with well-known window functions [10] for $\kappa(z)$, we determined the optimum voltage set. In Fig. 3, the calculated spectral response is shown for a Kaiser-type window function discretized into 20 sections (see Fig. 7). For comparison, the spectral response for homogenous coupling is also shown with sidelobes of about $-10$ dB below the maximum transmission. In contrast, a coupling strength function that approximates a Kaiser-type window function leads to a filter response with sidelobe suppression better than 40 dB.

Wavelength tuning of the filter is possible by imposing a phase shift $\Delta\phi$ of the coupling strength between subsequent sections of the filters [2]. By such an additional phase shift, the wavelength of maximum conversion is shifted. This tuning can be realized by a proper adjustment of the in-phase and quadrature voltages according to (5) and (6). In Fig. 4, calculated spectral responses are shown assuming a Kaiser-type window function for various relative phase shifts between subsequent sections. (The interaction length was discretized into 16 sections, allowing a direct comparison with the experiments described in Section V.) With increasing phase shift, satellite peaks occur, which are about 25 nm separated from the central peak [2]. This separation increases with shorter length of the electrode sections. However, within a spectral range of about 10 nm, the filter can be tuned without getting satellite peaks of more than $-10$ dB height.

An alternative tuning method is temperature tuning. Because of the temperature dependence of the refractive indexes, the
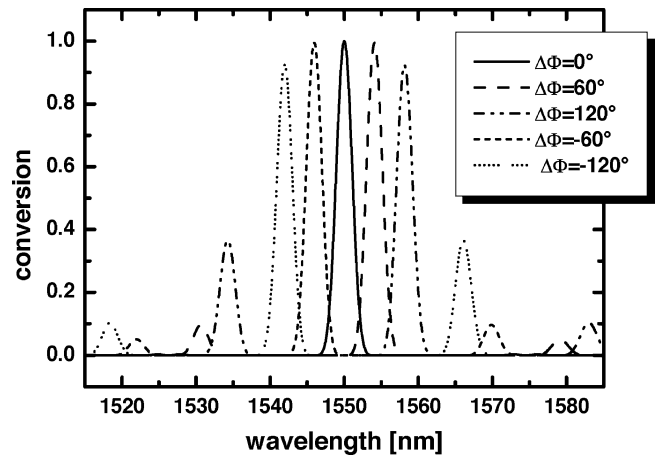


Fig. 4. Calculated tuning characteristics of a filter with 16 sections (Kaiser-type window). Between subsequent sections, a relative phase shift of $\Delta\phi$ is imposed.



Fig. 5. Photograph of the sample.

wavelength at which phase matching is obtained can be shifted with a slope of about $-0.6$ nm/°C. However, for most applications, the previously described electro-optic tuning is preferable as it promises a fast tuning speed.

## IV. SAMPLE FABRICATION

Optical waveguides were fabricated by an indiffusion of 7 $\mu$m wide and 100 nm thick Ti-stripes into X-cut LiNbO$_3$. The diffusion was performed at 1060 °C for 9 h. Prior to the electrode fabrication, a SiO$_2$ buffer layer of 500 nm thickness was deposited on the sample surface. Subsequently, 500 nm thick gold electrodes were evaporated according to the structure shown in Fig. 2 with a periodicity of $\Lambda = 21.7$ $\mu$m and a duty cycle of 50%. The sample has an overall length of 50 mm. In order to suppress spurious reflections at the end faces, an antireflection (AR) coating for the 1.55 $\mu$m spectral region was deposited onto the end faces.

Investigation of the waveguides in the spectral range around 1.55 $\mu$m revealed that they are monomode, and the losses are 0.1 (TM polarization) and 0.4 dB/cm (TE), respectively.

Fig. 5 shows a photograph of the sample. It is mounted on a copper holder, which is temperature stabilized at 40 °C with about 0.1 °C accuracy. Twenty electrode sections are connected via bonding wires to small strips of a printed circuit board beside the sample.
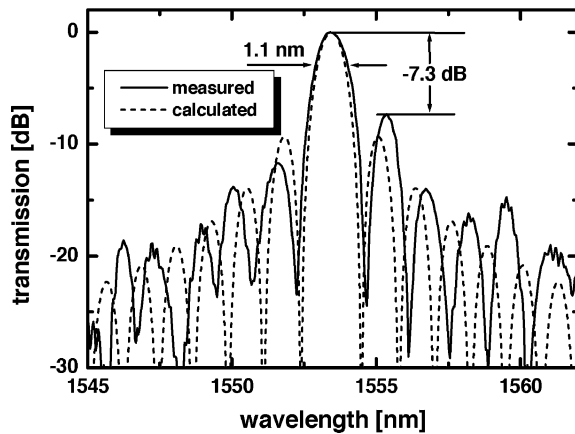
Fig. 6.   Measured (solid line) and calculated (dashed line) spectral response of the filter with homogenous coupling.

## V. EXPERIMENTAL RESULTS

In the optical setup, the amplified spontaneous emission from an Erbium-doped fiber amplifier is used as a broadband light source. The sample is mounted between (external) polarizers. The overall device acts either as bandpass or notch filter if the rear polarizer is adjusted to transmit the converted or the unconverted light, respectively. End-face coupling using lenses with 10 mm focal length is used at the input and output sides of the sample. The transmitted light is fed to an optical spectrum analyzer with 0.1 nm resolution. A computer-controlled programmable voltage supply with up to 32 channels delivering $-50$ V,..., $+50$ V was used to drive the electro-optic converter sections.

In the first experiment, a constant voltage $U$ was applied to all contacted in-phase electrodes (20 sections). Operating the device as notch filter at $U = 11.2$ V, a complete conversion was obtained at the phase-matched wavelength of 1553.4 nm. The corresponding measured spectral bandpass response is shown in Fig. 6. The transmission at the phase-matched wavelength has been normalized to 0 dB. (This value is also taken as reference value for all transmission curves shown in Figs. 7–10.)

Because of inhomogeneities of the waveguide structure, the shape of the spectral characteristics differs from the ideally expected $\mathrm{sinc}^2$-function, which is also plotted in the diagram. The spectral bandwidth of the measured curve is 1.1 nm and the largest sidelobe is 7.3 dB below the maximum transmission.

In order to suppress the sidelobes, the voltages applied to the in-phase electrodes were modified to approximate a Kaiser-type window function as discussed in Section III. In Fig. 7 (top diagram), the corresponding voltages applied to the 20 electrodes are shown. Fig. 7 (bottom diagram) shows the resulting measured and calculated spectral responses. While the sidelobes are now strongly suppressed (the largest sidelobe of the measured characteristic is about 20.3 dB below maximum transmission), the spectral 3 dB bandwidth, on the other hand, increases to 2.3 nm, which is slightly larger than the predicted half-width of 2.1 nm.

Tuning of the filter as discussed in Section III could be also verified. For this experiment, we used all the 32 available
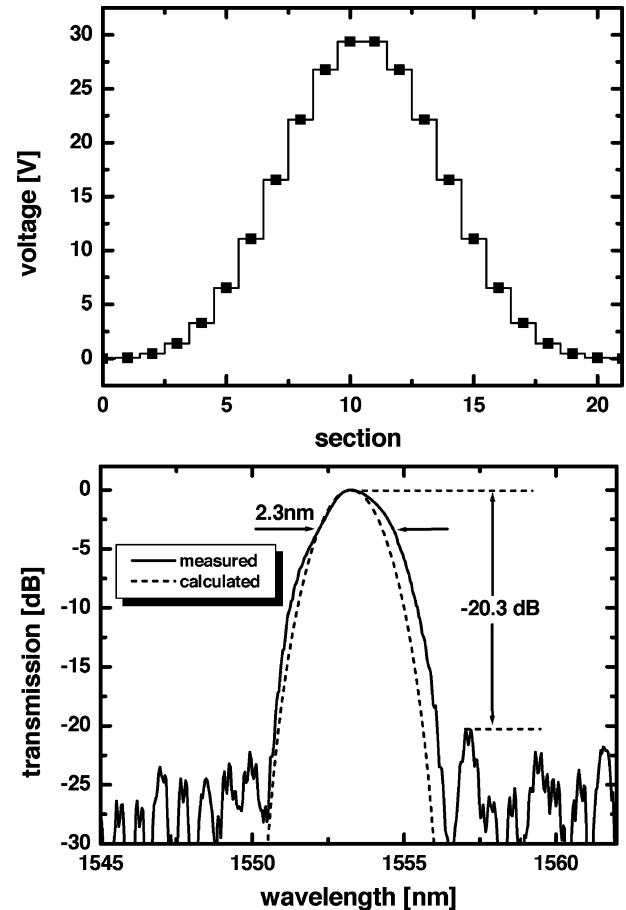


Fig. 7.   Filter with strong sidelobe suppression. (Top diagram) Voltages applied to the in-phase electrodes of the 20 sections, and (bottom diagram) measured and calculated corresponding spectral responses.
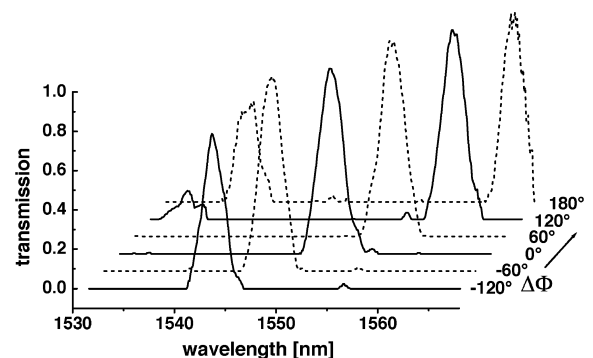


Fig. 8.   Measured tuning characteristics of a 16-sections filter with Kaiser-type coupling strength. The different curves are obtained by imposing a phase shift of $\Delta\Phi$ between subsequent sections.

voltage channels to drive in-phase and quadrature electrodes of 16 sections. In Fig. 8, the measured filter characteristics are shown for various relative phase shifts between subsequent sections. Filter tunability could be demonstrated as predicted from the theoretical results. With increasing $\Delta\Phi$, satellite peaks occur, which limit the useful tuning range of the filter. However, within a wavelength range of about 10 nm, the filter is tunable without severe deterioration of the filter performance due to these satellite peaks.
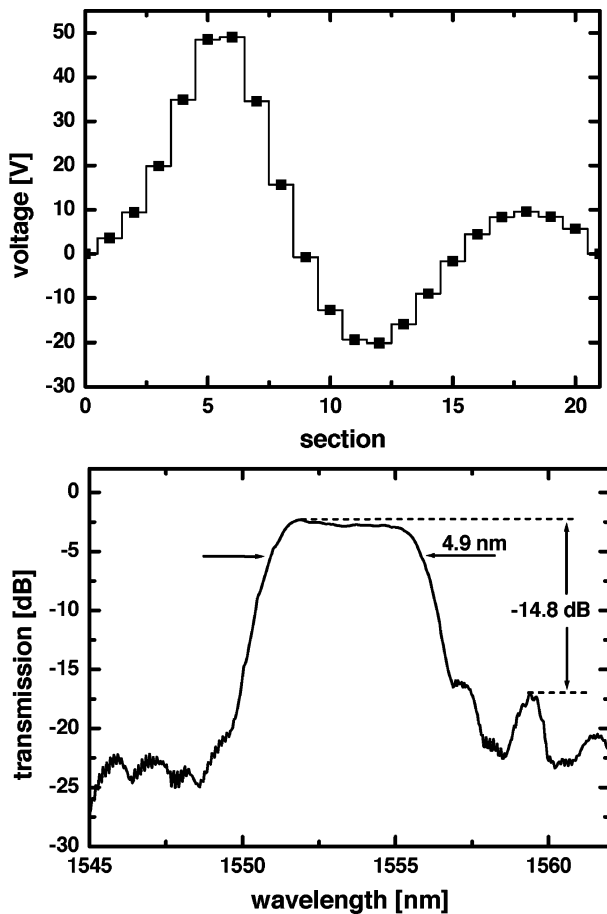
Fig. 9. Flat-top operation of the filter. (Top diagram) Voltages applied to the in-phase electrodes of the 20 sections, and (bottom diagram) measured corresponding spectral response.

have to be studied and optimized. Mainly due to the $SiO_2$ buffer layer between the electrodes and the $LiNbO_3$ surface, a temporal drift has been observed. Further systematic investigations to mitigate such effects will be performed.

Another direction for further activities will be a polarization-independent operation. This can be achieved by using a polarization diversity scheme. Furthermore, the integration of polarizers or polarization splitters (for the polarization-independent device) to form a complete integrated optical circuit would be of great importance.

## REFERENCES

[1] *Wavelength Filters in Fibre Optics (Springer Series in Optical Science 123)*, H. Venghaus, Ed.. Berlin, Germany: Springer-Verlag, 2006.
[2] F. Heismann and R. Alferness, "Wavelength tunable electrooptic conversion in birefringent waveguides," *IEEE J. Quantum Electron.*, vol. QE-24, no. 1, pp. 83–93, Jan. 1988.
[3] W. Warzanskyj, F. Heismann, and R. C. Alferness, "Polarization independent electro-optically tunable narrowband wavelength filter," *Appl. Phys. Lett.*, vol. 53, pp. 13–15, 1988.
[4] H. Herrmann, D. Büchter, R. Ricken, and W. Sohler, "Integrated electro-optic filter with programmable spectral response," presented at the Eur. Conf. Integr. Opt. (ECIO 2007), Copenhagen, Denmark, Paper ThA1.
[5] Y. Ping, O. Eknoyan, and H. F. Taylor, "Electro-optic polarization converter with programmable spectral output in lithium niobate," *Opt. Commun.*, vol. 278, pp. 307–311, 2007.
[6] Y. Ping, O. Eknoyan, C. K. Madsen, and H. F. Taylor, "Programmable polarization-independent electrooptic matched bandpass filter utilizing symmetric branch beam splitters in $Ti:LiNbO_3$," *J. Lightw. Technol.*, vol. 25, pp. 2198–2205, 2007.
[7] R. C. Alferness and P. Cross, "Filter characteristics of codirectionally coupled waveguides with weighted coupling," *IEEE J. Quantum Electron.*, vol. QE-14, no. 11, pp. 843–847, Nov. 1978.
[8] H. Herrmann, U. Rust, and K. Schäfer, "Tapered acoustical directional couplers for integrated acousto-optical mode converters with weighted coupling," *J. Lightw. Technol.*, vol. 13, pp. 364–374, 1995.
[9] D. A. Smith and J. J. Johnson, "Sidelobe suppression in an acousto-optic filter with a raised-cosine interaction strength," *Appl. Phys. Lett.*, vol. 61, pp. 1025–1027, 1992.
[10] P. S. Cross and H. Kogelnik, "Sidelobe suppression in corrugated waveguide filters," *Opt. Lett.*, vol. 1, pp. 43–45, 1977.
[11] R. Noé, D. Sandel, S. Hinz, M. Yoshida-Dierolf, V. Mirvoda, G. Feise, H. Herrmann, R. Ricken, W. Sohler, F. Wehrmann, C. Glingener, A. Schöpflin, A. Färbert, and G. Fischer, "Integrated optical $LiNbO_3$ distributed polarisation mode dispersion compensator in 20 Gbit/s transmission system," *Electron. Lett.*, vol. 35, pp. 652–654, 1999.
[12] R. Noé, D. Sandel, and V. Mirvoda, "PMD in high-bit-rate transmission and means for its mitigation," *IEEE J. Sel. Topics Quantum Electron.*, vol. 10, no. 2, pp. 341–355, 2004.
[13] G.-H. Song and S.-Y. Shin, "Design of corrugated waveguide filters by the Gel'fand–Levitan–Marchenko inverse-scattering method," *J. Opt. Soc. Amer. A, Opt. Image Sci.*, vol. 2, pp. 1905–1915, 1985.
[14] K. A. Winick, "Design of grating-assisted waveguide couplers with weighted coupling," *J. Lightw. Technol.*, vol. 9, pp. 1481–1492, 1991.

Another example of a tailored spectral response obtained with the same programmable filter is shown in Fig. 9. Here, the device has been programmed to provide a (nearly) rectangular response, i.e., a flat-top characteristic. Such flat-top filters can be realized using a coupling strength that approximates a Butterworth function. In our case, we have chosen a coupling strength approximating a seventh-order Butterworth function. Because of the limited voltages available from our multichannel voltage supply, we could not obtain complete conversion. Maximum conversion is about $-2.9$ dB. The spectral 3 dB width is about 4.9 nm and the highest sidelobe $-14.8$ dB below the maximum conversion.

## VI. CONCLUSION

We have demonstrated an integrated electro-optic wavelength filter with a programmable spectral response. Bandpass filter characteristics with high sidelobe suppression and flat-top response have been experimentally demonstrated as well as tunability of the filter. The results are in good agreement with theoretical predictions.

Further work will concentrate on the improvement of the filter performance. In particular, the dynamical properties of the filter

**Harald Herrmann** received the Diploma degree in physics from the University of Hannover, Hanover, Germany, in 1984, and the Ph.D. degree (Dr.rer.nat.) from Paderborn University, Paderborn, Germany, in 1991.

In 1991, he joined the Applied Physics/Integrated Optics Group, Paderborn University, where he was involved in the study of nonlinear frequency conversion processes in integrated optical waveguides, and has been engaged in the development of integrated optical devices based on acoustooptic, electrooptic, or nonlinear optical interactions.

**Kai-Daniel Büchter** was born in 1981. He received the B.S. and M.S. degrees in physics in 2005 and 2007, respectively, from the University of Paderborn, Paderborn, Germany, where he is currently working toward the Ph.D. degree at the Center for Optoelectronics and Photonics Paderborn.

His research interests include electro-optic effects and nonlinear-optical frequency conversion in periodically poled lithium niobate waveguides for midIR applications.

**Raimund Ricken** received the Diploma degree in physics from the University of Essen, Essen, Germany, in 1982.

In 1983, he joined the Integrated Optics/Applied Physics Group, University of Paderborn, Paderborn, Germany, where he is currently responsible for the technology of integrated optical devices. He has more than 25 years of experiences in the fabrication technology of integrated waveguide devices in $LiNbO_3$.

**Wolfgang Sohler** received the Diplom-Physiker and Dr.rer.nat. degrees in physics from the University of Munich, Munich, Germany, in 1970 and 1974, respectively.

From 1975 to 1980, he was with the University of Dortmund, Germany, where he was involved in integrated optics. In 1980, he joined Fraunhofer Institut für Physikalische Messtechnik, Freiburg, Germany, as the Head of the Department of Fiber Optics. Since 1982, he has been with the University of Paderborn, Paderborn, Germany, as Professor of applied physics. His research interests include integrated optics, fiber optics, and laser physics. He is the author or coauthor of more than 250 journal and conference contributions, and of several book chapters.